Original Article for Thyroid

A novel diagnostic method for thyroid follicular tumors based on immunofluorescence analysis of p53-binding protein 1 expression: detection of genomic instability

Ryota Otsubo[1,2], Katsuya Matsuda[1], Zhanna Mussazhanova[1], Ayako Sato[1,2], Megumi Matsumoto[2], Hiroshi Yano[2], Masahiro Oikawa[3], Hisayoshi Kondo[4], Masahiro Ito[5], Akira Miyauchi[6], Mitsuyoshi Hirokawa[7], Takeshi Nagayasu[2], and Masahiro Nakashima[1]

[1] Department of Tumor and Diagnostic Pathology, Atomic Bomb Disease Institute, Nagasaki University, Nagasaki 852-8523, Japan

[2] Department of Surgical Oncology, Nagasaki University Graduate School of Biomedical Sciences, Nagasaki 852-8501, Japan

[3]Division of Breast Surgery, New-wa-kai Oikawa Hospital, Fukuoka 810-0014, Japan

[4] Biostatics Section, Division of Scientific Data Registry, Atomic Bomb Disease Institute, Nagasaki University Graduate School of Biomedical Sciences, Nagasaki 852-8523, Japan

[5] Department of Pathology, National Hospital Organization Nagasaki Medical Center, Nagasaki 856-8562, Japan

[6] Department of surgery, Kuma Hospital, Kobe, Hyogo 650-0011, Japan

[7] Department of Diagnostic Pathology and Cytology, Kuma Hospital, Kobe, Hyogo 650-0011, Japan

Corresponding Author: Masahiro Nakashima, M.D., Ph.D.
Department of Tumor and Diagnostic Pathology, Atomic Bomb Disease Institute, Nagasaki University, 1-12-4 Sakamoto, Nagasaki 852-8523, Japan
TEL: + 81-95-819-7105, FAX: +81-95-819-7108
E-mail: moemoe@nagasaki-u.ac.jp

Ryota Otsubo, M.D., Ph.D.

Department of Surgical Oncology, Nagasaki University Graduate School of Biomedical Sciences, Nagasaki 852-8501, Japan. E-mail: rotsubo@nagasaki-u.ac.jp

Katsuya Matsuda, C.T., Ph.D.

Department of Tumor and Diagnostic Pathology, Atomic Bomb Disease Institute, Nagasaki University, Nagasaki 852-8523, Japan. E-mail: katsuya@nagasaki-u.ac.jp

Zhanna Mussazhanova, M.D., Ph.D.

Department of Tumor and Diagnostic Pathology, Atomic Bomb Disease Institute, Nagasaki University, Nagasaki 852-8523, Japan. E-mail: ghannakz@mail.ru

Ayako Sato, M.D.

Department of Surgical Oncology, Nagasaki University Graduate School of Biomedical Sciences, Nagasaki 852-8501, Japan. E-mail: ay_dopey_smile@yahoo.co.jp

Megumi Matsumoto, M.D., Ph.D.

Department of Surgical Oncology, Nagasaki University Graduate School of Biomedical Sciences, Nagasaki 852-8501, Japan. E-mail: mmatsumoto@nagasaki-u.ac.jp

Hiroshi Yano, M.D., Ph.D.
Department of Surgical Oncology, Nagasaki University Graduate School of Biomedical Sciences, Nagasaki 852-8501, Japan. E-mail: hiroyano@nagasaki-u.ac.jp

Masahiro Oikawa, M.D., Ph.D.
Division of Breast Surgery, New-wa-kai Oikawa Hospital, Fukuoka 810-0014, Japan.
Email: oimasa@iris.dti.ne.jp

Hisayoshi Kondo, Ph.D.
Biostatics Section, Division of Scientific Data Registry, Atomic Bomb Disease Institute, Nagasaki University, Nagasaki 852-8523, Japan. E-mail: hkondo@nagasaki-u.ac.jp

Masahiro Ito, M.D., Ph.D.

Department of Pathology, National Hospital Organization Nagasaki Medical Center, Nagasaki 856-8562, Japan. E-mail: itohm@nagasaki-mc.com

Akira Miyauchi, M.D., Ph.D.

Department of Surgery, Kuma Hospital, Kobe, Hyogo 650-0011, Japan. E-mail: miyauchi@kuma-h.or.jp

Mitsuyoshi Hirokawa, M.D., Ph.D.

Department of Diagnostic Pathology and Cytology, Kuma Hospital, Kobe, Hyogo 650-0011, Japan. E-mail: mhirokawa@kuma-h.or.jp

Takeshi Nagayasu, M.D., Ph.D.

Department of Surgical Oncology, Nagasaki University Graduate School of Biomedical Sciences, Nagasaki 852-8501, Japan. E-mail: nagayasu@nagasaki-u.ac.jp

81 Masahiro Nakashima, M.D., Ph.D.

82 Department of Tumor and Diagnostic Pathology, Atomic Bomb Disease Institute,

83 Nagasaki University, Nagasaki 852-8523, Japan. E-mail: moemoe@nagasaki-u.ac.jp

84

85 **Running head:** 53BP1 in thyroid follicular tumors

86

87 **Keywords**: 53BP1, DNA damage response, genomic instability, immunofluorescence,

88 thyroid follicular tumors

89 **Abstract**

90 **Background:** The preoperative diagnosis of thyroid follicular carcinomas by fine-
91 needle aspiration cytology (FNAC) is almost impossible. We previously demonstrated
92 that p53-binding protein 1 (53BP1) expression, based on immunofluorescence (IF), can
93 serve as a valuable biomarker to estimate the malignant potential of various cancers.
94 53BP1 belongs to a class of DNA damage response molecules that rapidly localize to
95 the site of DNA double-strand breaks (DSBs), forming nuclear foci (NF). This study
96 aimed to elucidate the utility of 53BP1 NF expression as a biomarker to differentiate
97 follicular tumors (FTs).
98 **Methods:** We analyzed associations between 53BP1 expression based on IF and
99 histological types of FTs using 27 follicular adenomas (FAs), 28 minimally invasive
100 follicular carcinomas (MFCs), and 14 widely invasive FCs (WFCs). Furthermore, our
101 study clarified the relationship between 53BP1 NF and copy number aberrations
102 (CNAs) based on array comparative genomic hybridization (aCGH), a hallmark of
103 genomic instability (GIN).

Results: This study demonstrated differences in 53BP1 NF expression between FA and FC. The incidence of 53BP1 at NF significantly increased with FT progression in the following order: normal follicle < FA < MFC < WFC. In contrast, no significant differences were observed in CNAs among the FT samples. Furthermore, there was no significant correlation between CNAs and 53BP1 at NF in FTs. Thus, based on a comparison of these two indicators of GIN, 53BP1 NF (by IF) was better able to estimate the malignancy of FTs compared to CNA (by aCGH). Interestingly, IF revealed the heterogenous distribution of 53BP1 NF, which occurred more frequently in the invasive or subcapsular area than in the center of the tumor, suggesting intra-tumor heterogeneity of GIN in FTs.

Conclusions: We propose that IF analysis of 53BP1 expression could be a novel diagnostic method to estimate the malignant potential of FTs. Because 53BP1 NF reflect DNA DSBs, we hypothesize that the incidence of 53BP1 at NF can represent the level of GIN in tumor cells.

Introduction

Follicular carcinoma (FC) is the second most common type of thyroid carcinoma and must be differentiated from more common follicular adenoma (FA) (1). It is almost impossible to preoperatively diagnose thyroid follicular tumors (FTs) by fine-needle aspiration cytology (FNAC), because the criteria for distinguishing these lesions are based on histological evidence such as capsular/vascular invasion or metastasis, and not on cytologic features, as is the case for papillary thyroid carcinoma (PTC) (2,3). According to the Bethesda System for Reporting Thyroid Cytology, almost all FCs are of category III, which is defined as atypia of undetermined significance or follicular lesions of undetermined significance (AUS/FLUS), or category IV, which is defined as follicular neoplasm or suspicious for follicular neoplasm (FN/SFN); for these categories, the estimated risk of malignancy is 5–15% or 15–30%, respectively (4). Thus, to avoid unnecessary surgery, several patients with FC, especially those cases including vascular invasion, are required to undergo a complementary total thyroidectomy after a preceding histological diagnostic hemithyroidectomy.

Several molecular techniques have been proposed for the preoperative diagnosis of FTs (5-7), but there is no decisive method that can clearly distinguish benign tumors from malignancy. We previously demonstrated that an immunofluorescence (IF)-based method to detect p53-binding protein 1 (53BP1) expression can serve as a valuable molecular marker to estimate the malignant potential of various cancers including thyroid (8), skin (9), and uterine cervix (10). 53BP1 belongs to a family of evolutionarily conserved DNA damage response (DDR) molecules that are rapidly recruited to the site of DNA double-strand breaks (DSBs) as a downstream effector of γ-H2AX (11); these molecules then form nuclear foci (NF) to co-operatively activate p53 with other kinases (12-14). The recruitment of 53BP1 protects the damaged end of DNA from undergoing resection, which in turn prevents error-free homologous recombination (HR) repair and instead promotes error-prone non-homologous end-joining (NHEJ) (15-19). The expression of 53BP1 at NF has been found to reflect ionizing radiation-induced DSBs, which increase linearly with radiation dose (12). Genomic instability (GIN) is considered an important hallmark of malignant tumors and is occasionally evident in the precancerous stage of carcinogenesis. Given that one

manifestation of GIN is induction of the endogenous DDR (20), we proposed that 53BP1 NF, based on IF, might be a useful tool to estimate the level of GIN, as well as the malignant potential of human tumors.

To elucidate the utility of 53BP1 expression as a biomarker to differentiate thyroid FTs, this study analyzed associations between 53BP1 expression and histological types such as FAs, minimally invasive FCs (MFCs), and widely invasive FCs (WFCs). Furthermore, to validate the significance of 53BP1 NF in estimating GIN among FTs, our study also clarified the relationship between 53BP1 NF and copy number aberrations (CNAs) detected by array comparative genomic hybridization (aCGH), which is a well-known hallmark of GIN during carcinogenesis (13, 14).

Materials and Methods

Thyroid tissues

A total of 69 surgically-resected, formalin-fixed, paraffin-embedded (FFPE) thyroid FTs including 27 conventional-type FAs, 28 MFCs, and 14 WFCs were used in this study. The diagnoses of all patients were histologically and macroscopically

166 confirmed by a pathologist specializing in thyroid oncology (MH or MN). Any
167 suspicious cases were excluded from our analysis. As a normal control, seven non-
168 tumorous follicular tissues surrounding FTs were also evaluated. Clinicopathologic
169 factors and preoperative cytological diagnoses of these cases are summarized in Table
170 1. This study was retrospectively conducted in accordance with the tenets of the
171 Declaration of Helsinki and approved by the institutional ethical committee for medical
172 research at Nagasaki University (approval date: July 24, 2015; #1506265). Following
173 the guidelines of the ethical committee's official informed consent and disclosure
174 system, detailed information regarding the study is available on our website
175 (http://www-sdc.med.nagasaki-u.ac.jp/pathology/research/index.html). Patients were
176 able to opt out of the study by following the instructions on the faculty website. All
177 samples were resected from patients at the Nagasaki University Hospital from 1994 to
178 2012 and the Kuma Hospital from 2010 to 2012.
179
180 ***IF analysis of 53BP1 expression***

After antigen retrieval by microwaving in citrate buffer, deparaffinized 4-μm sections were preincubated with 10% normal goat serum. Tissue sections were then incubated with an anti-53BP1 rabbit polyclonal antibody (A300-272A, Bethyl Labs, Montgomery, TX) at a 1:200 dilution for 1 h at room temperature. The slides were subsequently incubated with Alexa Fluor 488-conjugated goat anti-rabbit antibody (Molecular Probes Inc., Eugene, OR, USA). Specimens were counterstained with 4′,6-diamidino-2-phenylindole dihydrochloride (DAPI; Vysis Inc., Downers Grove, IL, USA), analyzed, and photographed using a High Standard All-in-One Fluorescence Microscope (Biorevo BZ-9000; KEYENCE Japan, Osaka, Japan) in Z-stack mode, accumulating images from 20 to 30 slices. Signals were analyzed from more than 15 viewing areas of subcapsular parts per case at a 1,000-fold magnification, as shown in Figure 1A. The 53BP1 immunoreactivity pattern was classified into three types based on the number and size of NF as follows: (i) stable type: faint nuclear staining, (ii) low DDR type: one or two discrete NF, (iii) high DDR type: three or more discrete NF, or discrete NF that are larger than 1.0 μm in the minor axis (Fig. 1B). The percentage of

196 follicular cells expressing each type of 53BP1 staining pattern was calculated for each
197 case.
198
199 ***Validation of IF analysis of 53BP1 expression using FFPE tissues***
200 We also performed IF analysis of 53BP1 expression to determine whether 53BP1
201 NF can be specifically detected in FFPE sections using thyroid tissues after irradiation.
202 Seven-week-old male Wistar rats were used for this. All animals received whole-body
203 irradiation using a Toshiba ISOVOLT TITAN32 X-ray, at 200 kV and a dose rate of
204 0.5531 Gy/min. Two doses of 0.1 and 4 Gy were administered. Two rats in each dose
205 group were sacrificed by deep anesthesia 2 h after irradiation. Each thyroid gland was
206 resected and immersed in neutral-buffered formalin, and routinely embedded in paraffin
207 blocks. Sections were used for IF according to the method described previously herein.
208 Control rats were not irradiated but were otherwise handled identically. This
209 experimental protocol was approved by the Institutional Animal Care and Use
210 Committee at Nagasaki University Animal Center (protocol No. #1610111343).
211

212 ***DNA extraction***

213 Genomic DNA was extracted from tumor areas in FFPE tissues as reported
214 previously (21). Tumor areas, identified using a guide slide stained with hematoxylin
215 and eosin, were microdissected from each FFPE block using 10×10-μm-thick-sections
216 and transferred into tubes. Paraffin removal was performed in 80% xylene; then, tissues
217 were washed twice with absolute ethanol and deparaffinized tissue pieces were
218 centrifuged at $15{,}000 \times g$ for 10 min at room temperature. After drying, pellets were
219 resuspended in 180 μl of buffer ATL (QIAamp DNA FFPE Kit, Qiagen, Hilden,
220 Germany) and digested with proteinase K for 72 h at 56 °C in a rotation oven with
221 periodic mixing and the addition of fresh proteinase K every 24 h. DNA was collected
222 using the QIAamp DNA FFPE Kit according to the manufacturer's instructions.
223 Extracted DNA was quantified using a NanoDrop ND-1000 spectrophotometer
224 (NanoDrop Technologies, Wilmington, DE, USA). The concentration of double-
225 stranded DNA (dsDNA) in each sample was quantitated using a Qubit dsDNA HS
226 Assay Kit (Life Technologies, Carlsbad, CA, USA), following the manufacturer's
227 instructions, as an indicator of DNA quality for aCGH analysis.

228

229 ***aCGH analysis***

230 aCGH analyses were performed as described previously (15). The Genomic DNA
231 ULS Labeling Kit (Agilent technologies, Santa Clara, CA, USA) was used to
232 chemically label 500 ng of DNA from tumor samples and reference female genomic
233 DNA (Promega, Madison, WI, USA) with Cy5 or Cy3 dyes, respectively, for 30 min at
234 85 °C, which was followed by purification using Agilent-KREApure™ columns. The
235 degrees of Cy5 and Cy3 labeling were calculated using a NanoDrop ND-2000
236 spectrophotometer (NanoDrop Technologies). Purified, labeled samples were then
237 combined and mixed with human Cot-1 DNA (Invitrogen, Carlsbad, USA), Agilent 10×
238 Blocking Agent, and Agilent 2× Hybridization Solution. Prior to array hybridization,
239 hybridization mixtures were denatured at 95 °C for 3 min and incubated at 37 °C for 30
240 min. An Agilent CGH block was added, and samples were hybridized to the SurePrint
241 G3 Human CGH 8×60 K Microarray, which contains eight identical arrays consisting of
242 ~63,000 in situ synthesized 60-mer oligonucleotide probes that span coding and
243 noncoding sequences with an average spatial resolution of ~54 kb. Hybridization was

carried out at 65 °C for 40 h before washing in Agilent Oligo aCGH Wash Buffer 1 at room temperature for 5 min; this was followed by washing in Agilent Oligo aCGH Wash Buffer 2 at 37 °C for 1 min. Scanning and image analysis were performed using an Agilent DNA Microarray Scanner. Feature Extraction Software (version 9.5) was used for data extraction from raw microarray image files. The Agilent Genomic Workbench (version 6.5) was used to visualize, detect, and analyze chromosomal patterns using an Aberration Detection Method-2 algorithm with the threshold set to 5.5. The derivative log ratio spread (DLRSpread) of each sample, which estimates the log ratio of noise by calculating the spread of log ratio differences between consecutive probes along all chromosomes, was used as an indicator of quality for aCGH analysis. A copy number gain was defined as a $\log_2$ ratio > 0.30 and a copy number loss was defined as a $\log_2$ ratio < −0.30.

Statistical analysis

Kruskal-Wallis or Cochran-Armitage tests were used to assess clinicopathologic factors of patients in this study. The Jonckheere-Terpstra test was used to assess

associations between the histological type of FTs (WFC, MFC, FA) and the results of preoperative cytology, and to assess differences in the level of 53BP1 expression or the total length of CNA by aCGH and the histological type of FTs. Spearman's correlation coefficients based on rank tests were used to assess the correlation between 53BP1 expression and the total length of CNA by aCGH. The PHREG procedure in SAS software (version 8.2; SAS Institute, Cary, NC, USA) was used for calculations. All tests were one-tailed, and a p-value < 0.05 was considered statistically significant.

Results

53BP1 expression in thyroid FTs

Representative images of the staining pattern of 53BP1 expression based on IF are shown in Figure 2. Our IF analysis of 53BP1 expression revealed the heterogeneous distribution of 53BP1 NF in FT sections. Specifically, we found more frequent expression of 53BP1 NF in the invasive front or subcapsular area as compared to that in the center portion of FTs, which were defined as shown in Figure 1. Therefore, 53BP1 expression was clarified at the site of the subcapsular areas of FTs. Based on these

276 results, we found a significant difference in the number of 53BP1 NF among different
277 histological types of FTs. Representative images of IF analysis of 53BP1 expression in
278 each FT histological type are presented in Figure 3. The median incidences of follicular
279 cells expressing 53BP1 NF were 6.9, 20.9, 28.3, and 36.4% in non-tumor follicles
280 (NTFs), FAs, MFCs, and WFCs, respectively. Furthermore, the median incidences of
281 follicular cells expressing the high DDR type were 0, 4.3, 6.4, and 9.9% in NTFs, FAs,
282 MFCs, and WFCs, respectively. Statistical analysis revealed a significant association
283 between 53BP1 NF/high DDR type and the histological type of FTs ($P < 0.001$, Fig. 4
284 and 5, respectively). The incidence of 53BP1 NF and high DDR type was significantly
285 increased with disease progression, in the following order NTFs, FAs, MFCs, and
286 WFCs. Adopting 3.1% as a cut-off value to distinguish FC from FA, the sensitivity and
287 specificity values were 90.5 and 77.8%, respectively (Fig. 5).
288
289 ***Validation of IF analysis for 53BP1 expression to detect DNA DSBs using FFPE***
290 ***sections***

As shown in Figure 6, our IF method for assessing 53BP1 expression clearly demonstrated NF in rat thyroid follicular cells after irradiation. No 53BP1 NF were found in non-irradiated rat thyroid glands, whereas the number of NF per cell was increased in dose-dependent manner, suggesting the specific detection of 53BP1 NF at sites of irradiation-induced DSBs in FFPE sections.

Correlation between type of 53BP1 expression and CNA by aCGH

We further examined the correlation between the type of 53BP1 expression and CNA as another hallmark of GIN. The degree of CNA was measured by aCGH in FFPE samples that met the DNA quality standard for this assessment, which included eight FAs, 10 MFCs, and nine WFCs in our series. The quality of aCGH data was considered acceptable, with a DLRSpread of 0.38 (0.20–0.69). The mean total numbers of CNAs were 25.7, 32.2, and 120.8 Mbp in FAs, MFCs, and WFCs, respectively, which was not significantly different based on FT histologic type ($p = 0.656$; Fig. 7). Furthermore, the correlation diagram comparing total number of CNAs and the proportion of tumor cells expressing 53BP1 NF is shown in Figure 8. Our statistical analysis of Spearman's

correlation coefficients based on the rank test revealed no significant correlation between the degree of CNA and 53BP1 NF or the high DDR type in FTs ($p = 0.226$ and 0.779, respectively). According to CNA at the single chromosome level, our results identified gain of 19p13.2 in four (50%) of eight FAs and gain of 8q24.3 in three of eight FAs (37.5%), six (60%) of 10 MFCs, and four (44%) of nine WFCs. However, significant correlations were not found between these alterations and the type of 53BP1 expression.

Discussion

The present study clearly demonstrated the existence of differences in 53BP1 expression at NF, particularly with respect to the incidence of tumor cells expressing the high DDR type, between FA and FC. The prevalence of the high DDR-type of 53BP1 immunoreactivity in follicular cells appeared to increase with FT progression. As evident in a validation experiment using irradiated rat thyroid glands, the presence of NF or DDR-type 53BP1 immunoreactivity was found to be concordant with the induction of DNA DSBs in follicular cells. Furthermore, our supplementary experiment

323 based on double IF analysis revealed the frequent co-localization of 53BP1 and γH2AX
324 NF in all examined FTs (10 cases), as well as in irradiated rat thyroid glands, suggesting
325 that endogenous activation of the DDR in tumor cells is a hallmark of GIN
326 (Supplementary figure). These results indicate a higher level of GIN in FCs as
327 compared to that in FAs. However, although CNAs (based on aCGH analysis), as
328 another hallmark of GIN and representing chromosomal loss and gain (13, 14, 21-23),
329 tended increase with FT progression, no significant difference was observed among FA,
330 MFC, and WFC samples. Previous reports also suggested no significant differences in
331 CNAs between FC and FA (24, 25). Furthermore, we could not demonstrate a
332 significant correlation between CNA levels and the DDR-type of 53BP1
333 immunoreactivity in FTs. Thus, upon comparing these two indicators of GIN, the
334 incidence of 53BP1 NF, reflecting endogenous DNA DSBs, based on IF, could be more
335 accurate in estimating the malignant potential of FTs, as compared to that with can-
336 based aCGH analysis. Interestingly, our IF analysis revealed the heterogenous
337 distribution of 53BP1 NF, which was more frequent in the invasive front or subcapsular
338 area, as compared to that in the center of the tumor, suggesting intra-tumor

heterogeneity of GIN in FTs. Thus, the intra-tumor heterogeneity based on CNA levels should be further elucidated. Actually, a previous study suggested the presence of tumor heterogeneity in FC based on aCGH (26).

According to the 2017 Bethesda System for Reporting Thyroid Cytology, in the cases of category III or IV, molecular testing is recommended to obtain further diagnostic information as usual management. Several molecular techniques were reportedly proposed for the preoperative diagnosis of FTs (5-7), but there is no critical method that can clearly distinguish between benign tumors and malignancy. Although there are several publications analyzing differences in CNAs among FTs by aCGH (25-32), to the best of our knowledge, any specific features that can distinguish FA or FC, which have been practically utilized, have not yet been identified. It has been reported that the gene-expression classifier Afirma® Thyroid FNA Analysis is practically available for the preoperative risk assessment of thyroid nodules with indeterminate FNAC (33). This diagnostic test is based on a microarray gene-expression assay measuring the expression of 167 genes using FNAC samples and was found to correctly identify 78 of 85 nodules as suspicious for malignancy (92% sensitivity), with a

355 specificity of 52% among 265 cytologically-indeterminate nodules (33). For nodules
356 classified as FN/SFN, the sensitivity was 90% and the specificity was 49%, suggesting
357 difficulties associated with predicting benign FT correctly using this assay (33). More
358 recently, the next-generation sequencing (NGS)-based ThyroSeq® using FNAC
359 samples was also made available (34). The ThyroSeq v2.1 panel detects known thyroid
360 cancer-associated molecular alterations including 14 genetic point mutations and 42
361 types of fusion genes (34). By analyzing 462 AUS/FLUS nodules of thyroid follicular
362 cells, this test revealed 31 (6.7%) were positive for mutations. Among them, 26 (84%)
363 were surgically removed and 20 (77%) malignant and six (23%) benign lesions were
364 histologically confirmed. Based on the results, all 20 malignant nodules were PC
365 including 18 follicular variants. The authors finally concluded that ThyroSeq v2.1 was
366 able to classify 20 of 22 cancers correctly, showing a sensitivity of 90.9%, a specificity
367 of 92.1%, a positive predictive value of 76.9%, and a negative predictive value of
368 97.2%, with an overall accuracy of 91.8%. Thus, although the accuracy of molecular
369 assays using FNAC samples has recently improved, it is still difficult to correctly

predict FCs of Bethesda category III (AUS/FLUS) or IV (FN/SFN), even by using modern techniques, and thus these methodologies require further improvements.

In summary, this retrospective study suggests that the incidence of high DDR-type 53BP1 immunoreactivity in FTs could be an attractive candidate biomarker to distinguish FC from FA. Indeed, when we adopted 3.1% as a cut-off value for the incidence of high DDR-type, this test could differentiate FC or FA among 69 FFPE FT samples with a sensitivity of 90.5% and a specificity of 77.8%. Although it is limited by the lower specificity, which means that a significant fraction of FA is not distinguishable, we propose that IF analysis of 53BP1 expression could represent a novel diagnostic method to estimate the malignant potential of thyroid FTs based on post-operative FFPE samples. Because 53BP1 NF reflect spontaneously occurring DNA DSBs, we hypothesize that the incidence of these foci can represent the level of GIN in tumor cells. IF analysis is associated with much lower cost and is technically easier compared to microarray gene-expression assays or NGS assays; it can also be used with both FFPE and FNAC samples. Thus, IF analysis of 53BP1 expression will not only be an auxiliary histologic technique to accurately diagnose FTs but also a novel technique

386 to make preoperative diagnoses based on FNAC from the invasive front or subcapsular
387 portion of FTs. Further studies using cytologic specimens are required to confirm this
388 notion in the near future.
389
390 **Acknowledgements**
391 This work was supported in part through the Atomic Bomb Disease Institute,
392 Nagasaki University, by a Grant-in-Aid for Scientific Research from the Japanese
393 Ministry of Education, Science, Sports and Culture (No. 24590414, No. 26461951), and
394 by the Program of the Network-Type Joint Usage/Research Center for Radiation
395 Disaster Medical Science.
396
397 **Author Disclosure Statement**
398 The authors have stated that they have no conflicts of interest.

References

1. Hemmer S, Wasenius VM, Knuutila S, Joensuu H, Franssila K 1998 Comparison of benign and malignant follicular thyroid tumours by comparative genomic hybridization. Br J Cancer **78**:1012–1017.

2. McHenry CR, Phitayakorn R 2011 Follicular adenoma and carcinoma of the thyroid gland. Oncologist **16**:585–593.

3. Suster S 2006 Thyroid tumors with a follicular growth pattern: problems in differential diagnosis. Arch Pathol Lab Med **130**:984–988.

4. Cibas ES, Ali SZ 2009 The Bethesda System for Reporting Thyroid Cytopathology. Thyroid **19**:1159–1165.

5. Sobrinho-Simões M, Preto A, Rocha AS, Castro P, Máximo V, Fonseca E, Soares P 2005 Molecular pathology of well-differentiated thyroid carcinomas. Virchows Arch **447**:787–793.

6. Foukakis T, Gusnanto A, Au AY, Höög A, Lui WO, Larsson C, Wallin G, Zedenius J 2007 A PCR-based expression signature of malignancy in follicular thyroid tumors. Endocr Relat Cancer **14**:381–391.

7. Nagar S, Ahmed S, Peeples C, Urban N, Boura J, Thibodeau B, Akervall J, Wilson G, Long G, Czako P 2014 Evaluation of genetic biomarker for distinguishing benign from malignant thyroid neoplasms. Am J Surg **207**:596–601.

8. Nakashima M, Suzuki K, Meirmanov S, Naruke Y, Matsuu-Matsuyama M, Shichijo K, Saenko V, Kondo H, Hayashi T, Ito M, Yamashita S, Sekine I 2008 Foci formation of p53-binding protein 1 in thyroid tumors: activation of genomic instability during thyroid carcinogenesis. Int J Cancer **122**:1082–1088.

9. Naruke Y, Nakashima M, Suzuki K, Matsuu-Matsuyama M, Shichijo K, Kondo H, Sekine I 2008 Alteration of p53-binding protein 1 expression during skin carcinogenesis: Association with genomic instability. Cancer Sci **99**:946–951.

10. Matusda K, Miura S, Kurashige T, Suzuki K, Kondo H, Ihara M, Nakajima H, Masuzaki H, Nakashima M 2011 Significance of p53-binding protein 1 nuclear foci in uterine cervical lesions: endogenous DNA double strand breaks and genomic instability during carcinogenesis. Histopathology **59**:441–451.

11. Wang B, Matsuoka S, Carpenter PB, Elledge SJ 2002 53BP1, a mediator of the DNA damage checkpoint. Science **298**:1435–1438.

431 12. Schultz LB, Chehab NH, Malikzay A, Halazonetis TD 2000 p53 binding protein 1
432 (53BP1) is an early participant in the cellular response to DNA double-strand breaks.
433 J Cell Biol **151**:1381–1390.
434 13. Negrini S, Gorgoulis VG, Halazonetis TD 2010 Genomic instability-an evolving
435 hallmark of cancer. Nat Rev Mol Cell Biol **11**:220–228.
436 14. Mondello C, Smirnova A, Giulotto E 2008 Gene amplification, radiation sensitivity
437 and DNA double-strand breaks. Mutat Res **704**:29–37.
438 15. Bunting SF, Callén E, Wong N, Chen H-T, Polato F, Gunn A, Bothmer A, Feldhahn
439 N, Fernandez-Capetillo O, Cao L, Xu X, Deng CX, Finkel T, Nussenzweig M, Stark
440 JM, Nussenzweig A 2010 53BP1 inhibits homologous recombination in Brca1-
441 deficient cells by blocking resection of DNA breaks. Cell **141**: 243–254.
442 16. Cao L, Xu X, Bunting SF, Liu J, Wang R-H, Cao LL, Wu JJ, Peng T-N, Chen J,
443 Nussenzweig A, Deng CX, Finkel T 2009 A selective requirement for 53BP1 in the
444 biological response to genomic instability induced by Brca1 deficiency. Mol Cell **35**:
445 534–541.
446 17. Chapman JR, Taylor MR, Boulton SJ. Playing the end game 2012 DNA double-

447 strand break repair pathway choice. Mol Cell **47**:497–510.

448 18. Kakarougkas A, Ismail A, Klement K, Goodarzi AA, Conrad S, Freire R, Shibata A,
449 Lobrich M, Jeggo PA 2013 Opposing roles for 53BP1 during homologous
450 recombination. Nucleic Acids Res **41**:9719–9731.

451 19. Zimmermann M, de Lange T 2014 53BP1: pro choice in DNA repair. Trends Cell
452 Biol **24**:108–117.

453 20. Suzuki K, Yokoyama S, Waseda S, Kodama S, Watanabe M 2003 Delayed
454 reactivation of p53 in the progeny of cells surviving ionizing radiation. Cancer Res
455 **63**:936–941.

456 21. Oikawa M, Yoshiura K, Kondo H, Miura S, Nagayasu T, Nakashima M 2011
457 Significance of genomic instability in breast cancer in atomic bomb survivors:
458 analysis of microarray-comparative genomic hybridization. Radiat Oncol **6**:168.

459 22. Kallioniemi OP, Kallioniemi A, Piper J, Isola J, Waldman FM, Gray JW, Pinkel D
460 1994 Optimizing comparative genomic hybridization for analysis of DNA sequence
461 copy number changes in solid tumors. Genes Chromosomes Cancer 10:231–243.

462 23. Mitelman F, Johansson B, Mertens F 2004 Fusion genes and rearranged genes as a
463 linear function of chromosome aberrations in cancer. Nat Genet **36**:331–334.
464 24. Roque L, Rodrigues R, Pinto A, Moura-Nunes V, Soares J 2003 Chromosome
465 imbalances in thyroid follicular neoplasms: a comparison between
466 follicular adenomas and carcinomas. Genes Chromosomes Cancer **36**:292–302.
467 25. Qureshi AA, Collins VP, Jani P 2013 Genomic differences in benign and malignant
468 follicular thyroid tumours using 1-Mb array-comparative genomic hybridisation. Eur
469 Arch Otorhinolaryngol **270**:325–335.
470 26. Da Silva L, James D, Simpson PT, Walker D, Vargas AC, Jayanthan J, Lakhani
471 SR, McNicol AM 2011 Tumor heterogeneity in a follicular carcinoma of thyroid: a
472 study by comparative genomic hybridization. Endocr Pathol **22**:103–107.
473 27. Hemmer S, Wasenius VM, Knuutila S, Joensuu H, Franssila K 1998 Comparison of
474 benign and malignant follicular thyroid tumours by comparative genomic
475 hybridization. Br J Cancer **78**:1012–1017.
476 28. Hemmer S, Wasenius VM, Knuutila S, Franssila K, Joensuu H 1999 DNA copy
477 number changes in thyroid carcinoma. Am J Pathol **154**:1539–1547.

29. Frisk T, Kytölä S, Wallin G, Zedenius J, Larsson C 1999 Low frequency of numerical chromosomal aberrations in follicular thyroid tumors detected by comparative genomic hybridization. Genes Chromosomes Cancer **25**:349–353.

30. Roque L, Rodrigues R, Pinto A, Moura-Nunes V, Soares J 2003 Chromosome imbalances in thyroid follicular neoplasms: a comparison between follicular adenomas and carcinomas. Genes Chromosomes Cancer **36**:292–302.

31. Rodrigues RF, Roque L, Rosa-Santos J, Cid O, Soares J 2004 Chromosomal imbalances associated with anaplastic transformation of follicular thyroid carcinomas. Br J Cancer **90**:492–496.

32. Castro P, Eknaes M, Teixeira MR, Danielsen HE, Soares P, Lothe RA, Sobrinho-Simões M 2005 Adenomas and follicular carcinomas of the thyroid display two major patterns of chromosomal changes. J Pathol **206**:305–311.

33. Alexander EK, Kennedy GC, Baloch ZW, Cibas ES, Chudova D, Diggans J, Friedman L, Kloos RT, LiVolsi VA, Mandel SJ, Raab SS, Rosai J, Steward DL, Walsh PS, Wilde JI, Zeiger MA, Lanman RB, Haugen BR 2012 Preoperative

493 diagnosis of benign thyroid nodules with indeterminate cytology. N Engl J Med
494 **367**:705–715.

495 34. Nikiforov YE, Carty SE, Chiosea SI, Coyne C, Duvvuri U, Ferris RL, Gooding
496 WE, LeBeau SO, Ohori NP, Seethala RR, Tublin ME, Yip L, Nikiforova MN 2015
497 Impact of the Multi-Gene ThyroSeq next-generation sequencing assay on cancer
498 diagnosis in thyroid nodules with atypia of undetermined significance/follicular
499 lesion of undetermined significance cytology. Thyroid **25**:1217–1223.

500

Figure legends

Fig. 1. Definition of anatomic sites of follicular tumors (**A**) and types of p53-binding protein 1 (53BP1) immunoreactivity (**B**) in this study. (**A**) The subcapsule was defined as an area within 2 mm of the inner line of the capsule and the center comprised an area more than 2 mm from the inner line of the capsule of tumors. (**B**) NF: nuclear foci; DDR: DNA damage response.

Fig. 2. Representative images of immunofluorescence analysis of p53-binding protein 1 (53BP1) expression in a follicular tumor. The incidence of 53BP1 nuclear foci was higher with invasion and in subcapsular areas compared to that in the center of the tumor or non-tumor thyroid.

Fig. 3. Immunofluorescence analysis of p53-binding protein 1 (53BP1) expression in follicular tumors of the thyroid. The incidence of 53BP1 nuclear foci in follicular cells was increasingly observed with follicular tumor progression based on the following

order: normal follicle (**A**), adenoma (**B**), minimally invasive carcinoma (**C**), widely invasive carcinoma (**D**).

Fig. 4. Comparison of median incidences of follicular cells expressing p53-binding protein 1 (53BP1) nuclear foci (NF) among follicular tumors (FTs) of the thyroid. The incidence of 53BP1 NF, which was measured in the subcapsular area of tumors, significantly ($p < 0.001$) increased in the order of follicular adenoma (FA), minimally invasive follicular carcinoma (MFC), and widely invasive follicular carcinoma (WFC).

Fig. 5. Comparison of median incidences of follicular cells expressing the high DNA damage response (DDR)-type of p53-binding protein 1 (53BP1) among follicular tumors (FTs) of the thyroid. The incidence of high DDR-type 53BP1 expression, which was measured in the subcapsule areas of tumors, significantly ($p < 0.001$) increased in the order of follicular adenoma (FA), minimally invasive follicular carcinoma (MFC), and widely invasive follicular carcinoma (WFC). Upon adopting a 3.1% cut-off value

for the incidence of the high DDR-type, this model could differentiate FC or FA among 69 FT cases with a sensitivity of 90.5% and a specificity of 77.8%.

Fig. 6. Immunofluorescence analysis of p53-binding protein 1 (53BP1) expression in irradiated rat thyroid tissues to detect DNA double strand breaks (DSBs) using formalin-fixed paraffin-embedded sections. No 53BP1 nuclear foci (NF) were observed in non-irradiated thyroid tissues, whereas the number of NF per cell was increased with irradiation in a dose-dependent manner.

Fig. 7. Comparison of the mean total number of copy number aberrations (CNAs) by array comparative genomic hybridization among follicular tumors (FTs) of the thyroid. No significant differences in CNAs were observed among histologic types of FTs including follicular adenoma (FA), minimally invasive follicular carcinoma (MFC), and widely invasive follicular carcinoma (WFC) ($p = 0.656$).

Fig. 8. Diagram of the correlation between total number of copy number aberrations (CNAs), based on array comparative genomic hybridization, and the incidence of tumor cells expressing p53-binding protein 1 (53BP1) nuclear foci (NF) in follicular tumors (FTs). No significant correlation between the number of CNAs and the expression of 53BP1 NF or the high DNA damage response (DDR)-type was observed in FTs including follicular adenoma (FA), minimally invasive follicular carcinoma (MFC), and widely invasive follicular carcinoma (WFC) ($p = 0.226$ and 0.779, respectively).

Supplementary Figure. Co-localization of 53BP1 (green) and γH2AX (red) nuclear foci in follicular carcinoma (upper and middle panels) and in rat thyroid follicular cells 2 h after 4-Gy irradiation (lower panels), as assessed by double-label immunofluorescence. The scale bar indicates 20 μm. The scale bar in the inset indicates 2 μm.

Figure 1

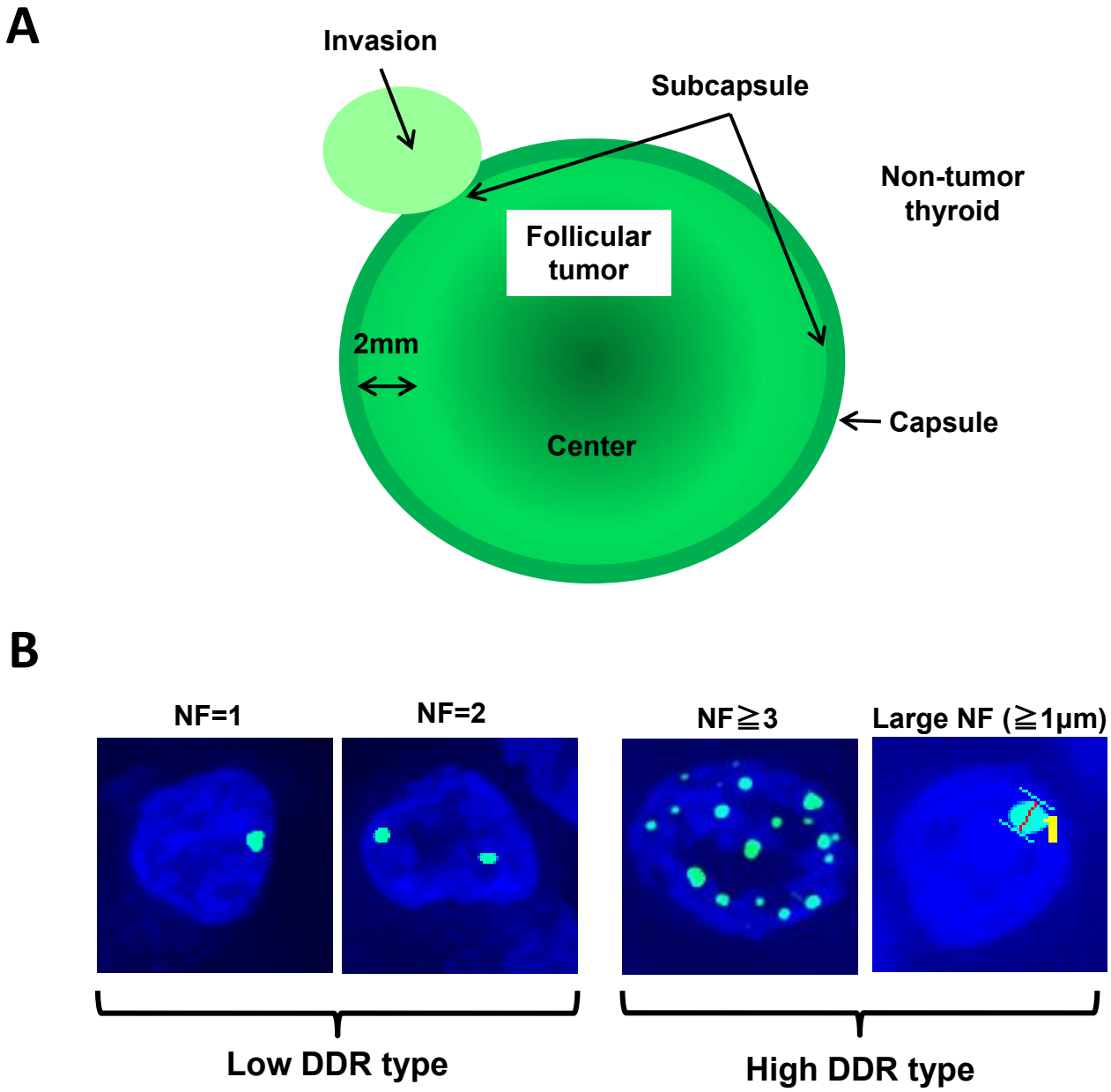
A
Invasion
Subcapsule
Non-tumor thyroid
Follicular tumor
2mm
Capsule
Center
B
NF=1
NF=2
NF≧3
Large NF (≧1μm)
Low DDR type
High DDR type

Figure 2

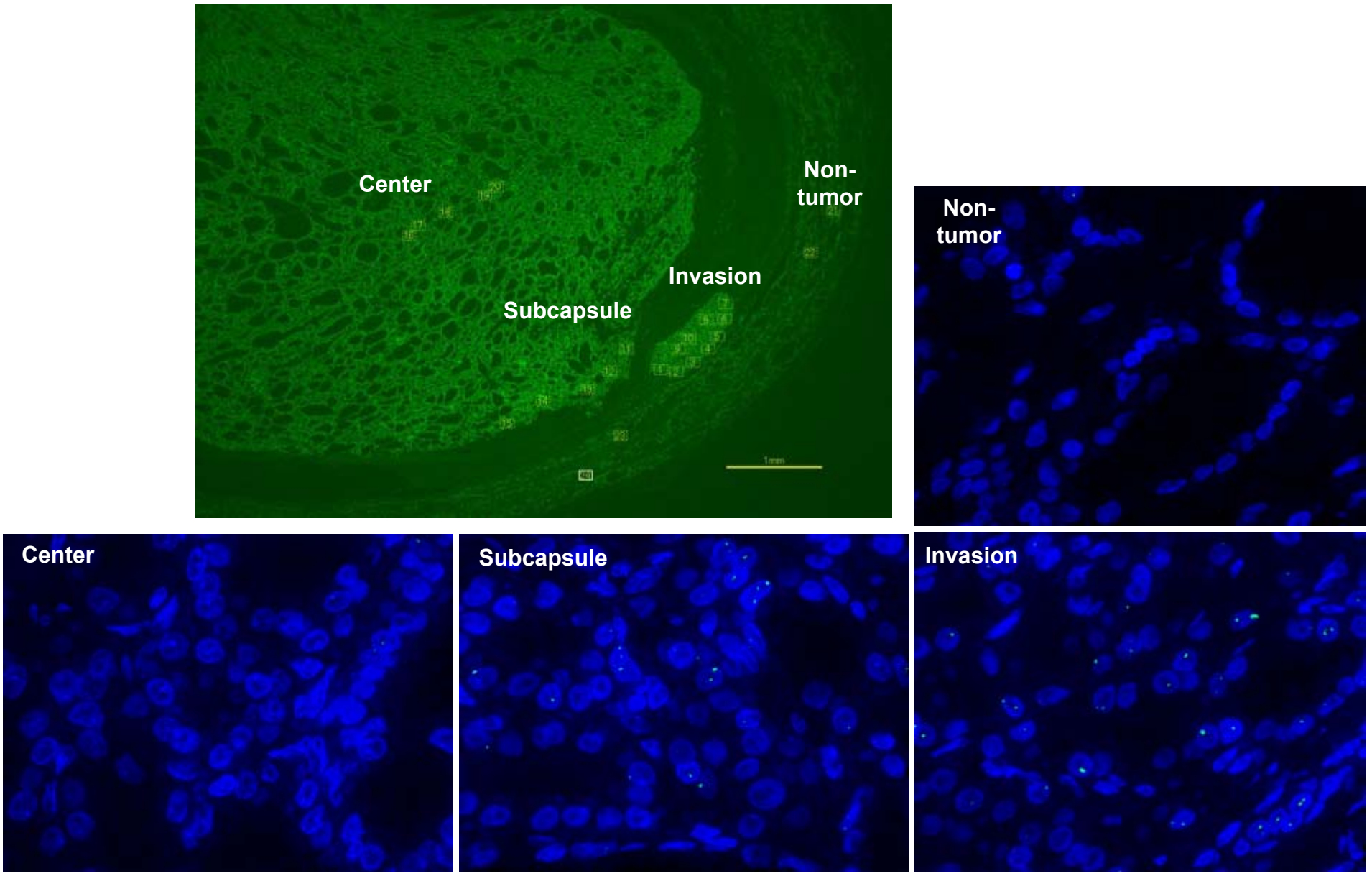
Center
Non-
tumor
Invasion
Subcapsule
Non-
tumor
Center
Subcapsule
Invasion

Figure 3

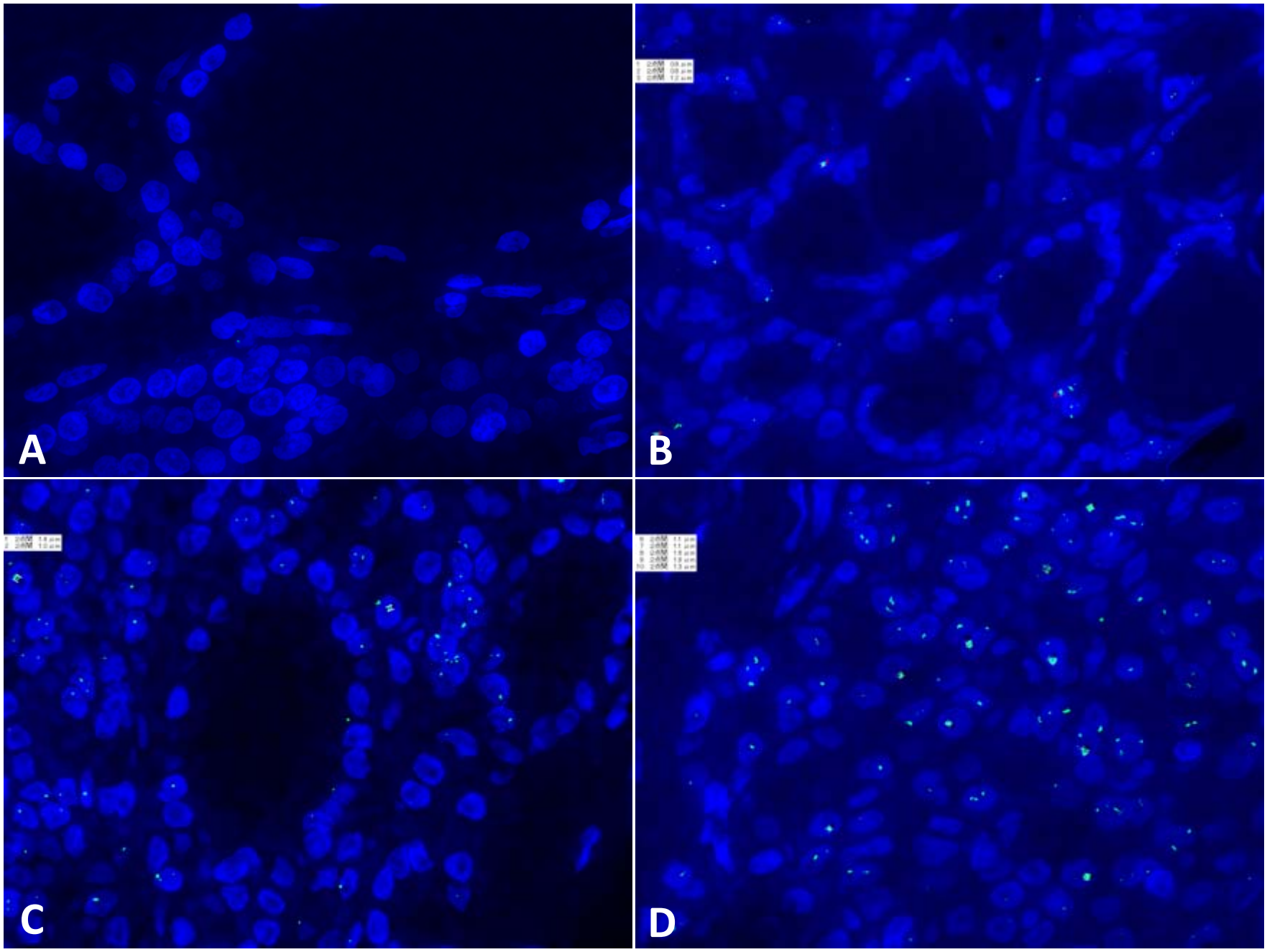

Figure 4

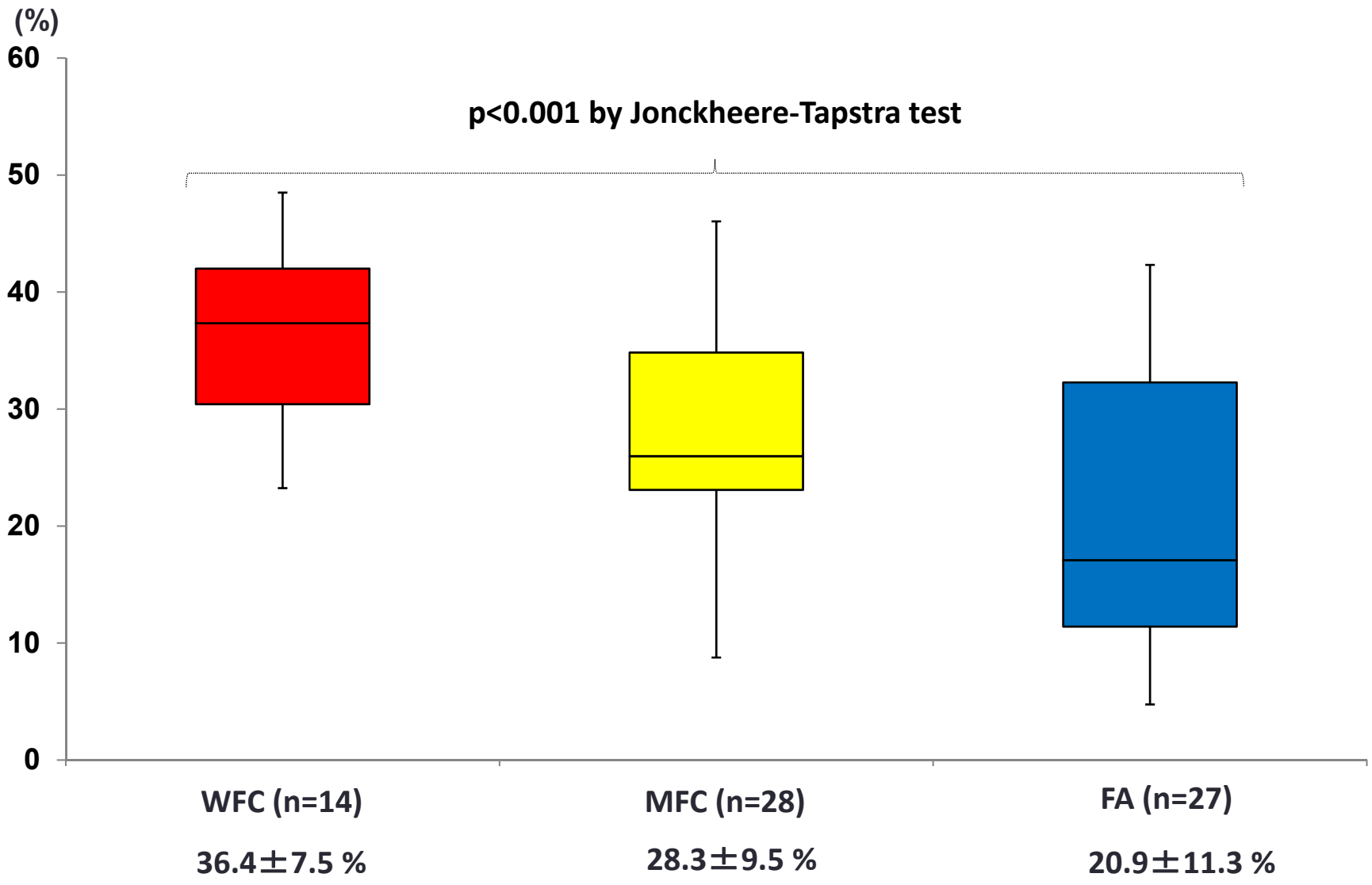
(%)
60
50
40
30
20
10
0
p<0.001 by Jonckheere-Tapstra test
WFC (n=14)
36.4±7.5 %
MFC (n=28)
28.3±9.5 %
FA (n=27)
20.9±11.3 %

Figure 5

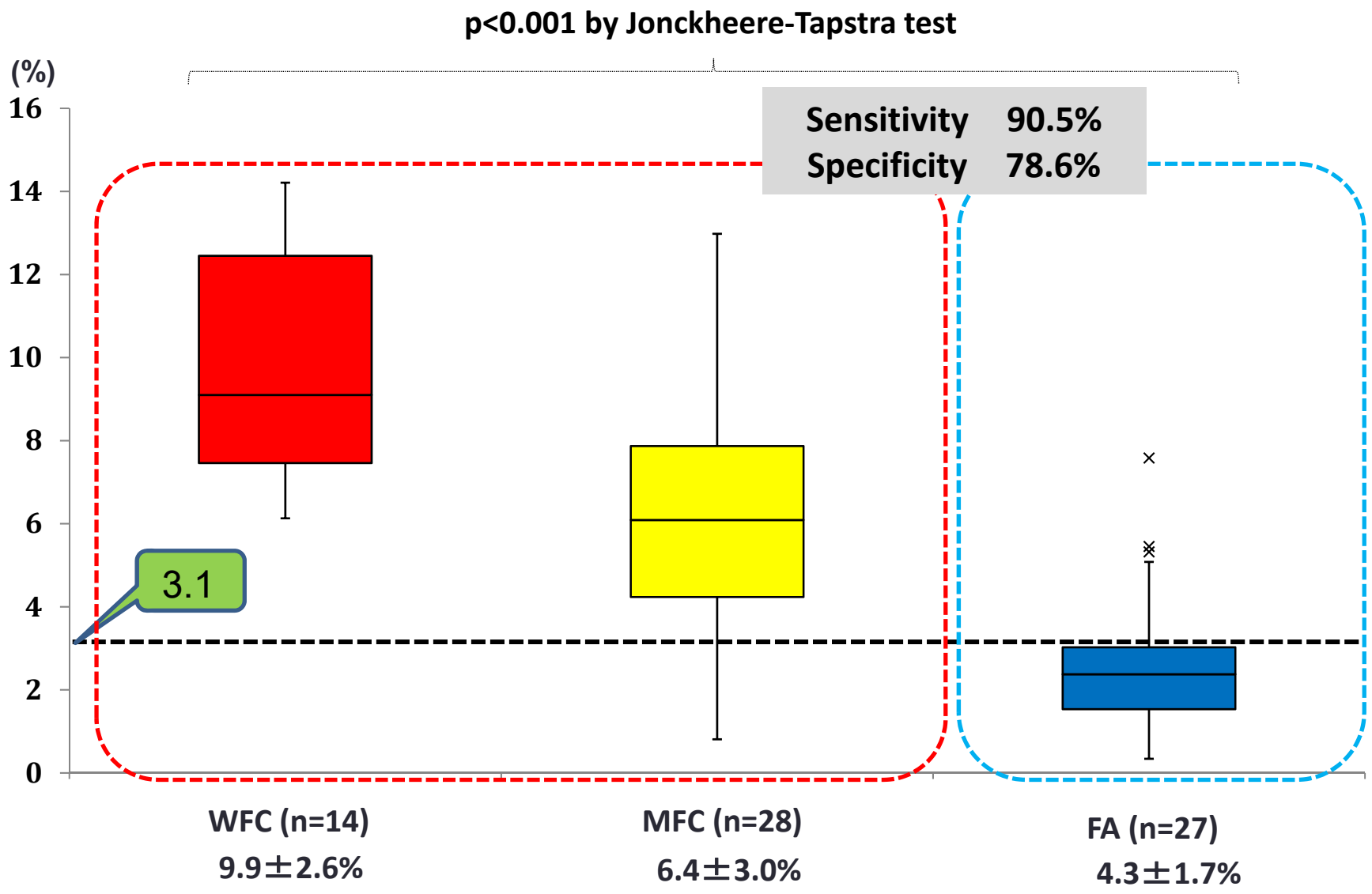
p<0.001 by Jonckheere-Tapstra test
(%)
16
14
12
10
8
6
4
2
0
Sensitivity 90.5%
Specificity 78.6%
3.1
WFC (n=14)
9.9±2.6%
MFC (n=28)
6.4±3.0%
FA (n=27)
4.3±1.7%

Figure 6

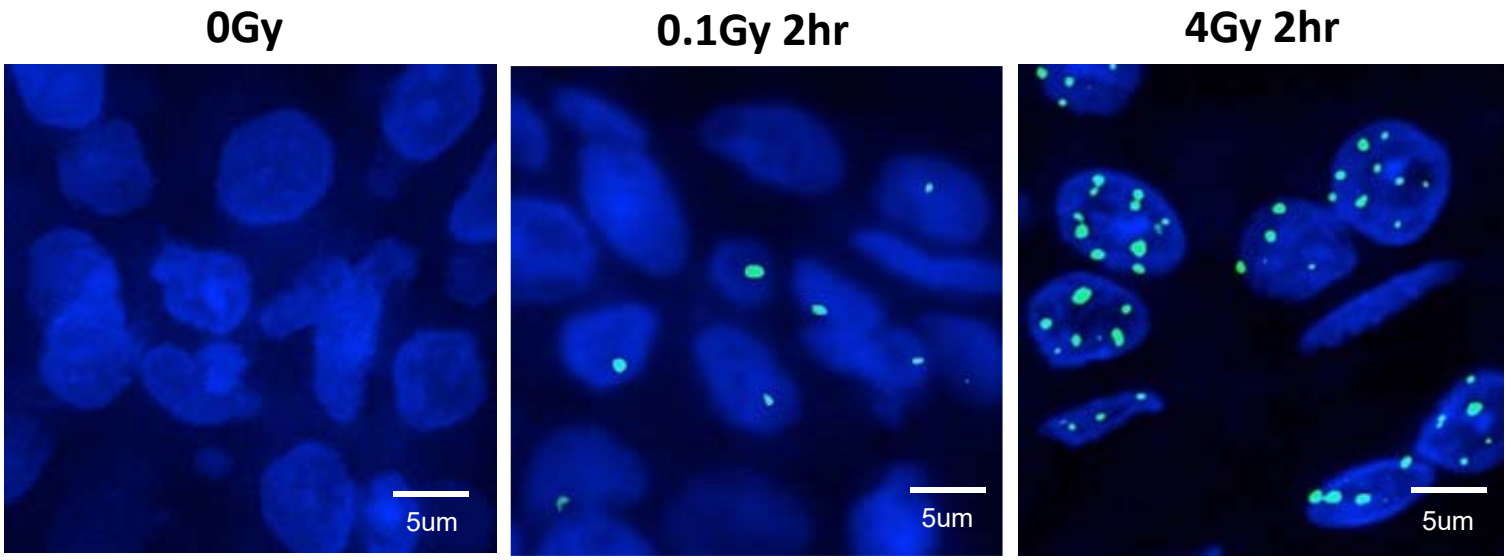

Figure 7

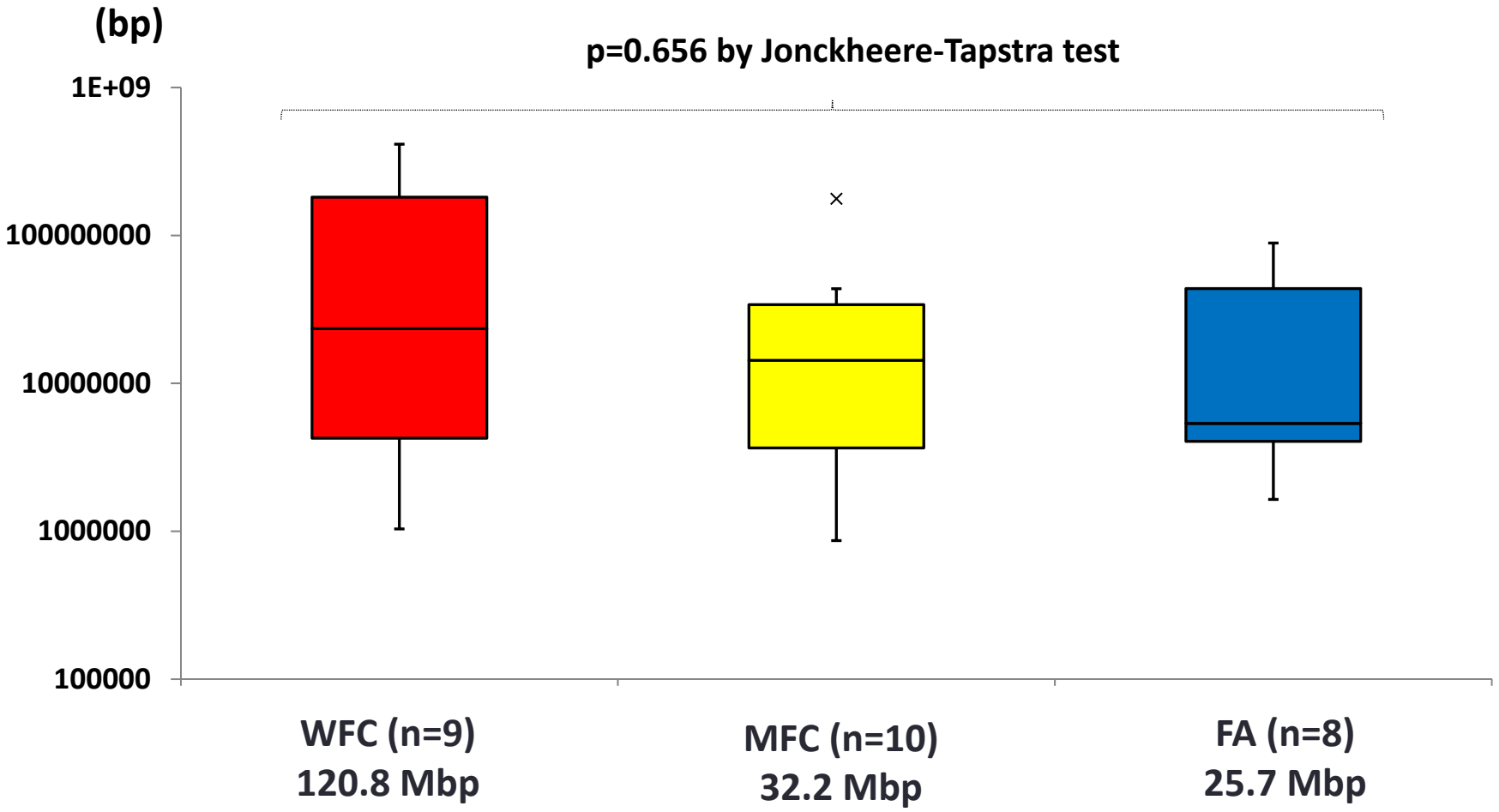
(bp)
p=0.656 by Jonckheere-Tapstra test
1E+09
100000000
10000000
1000000
100000
WFC (n=9)
120.8 Mbp
MFC (n=10)
32.2 Mbp
FA (n=8)
25.7 Mbp

Figure 8

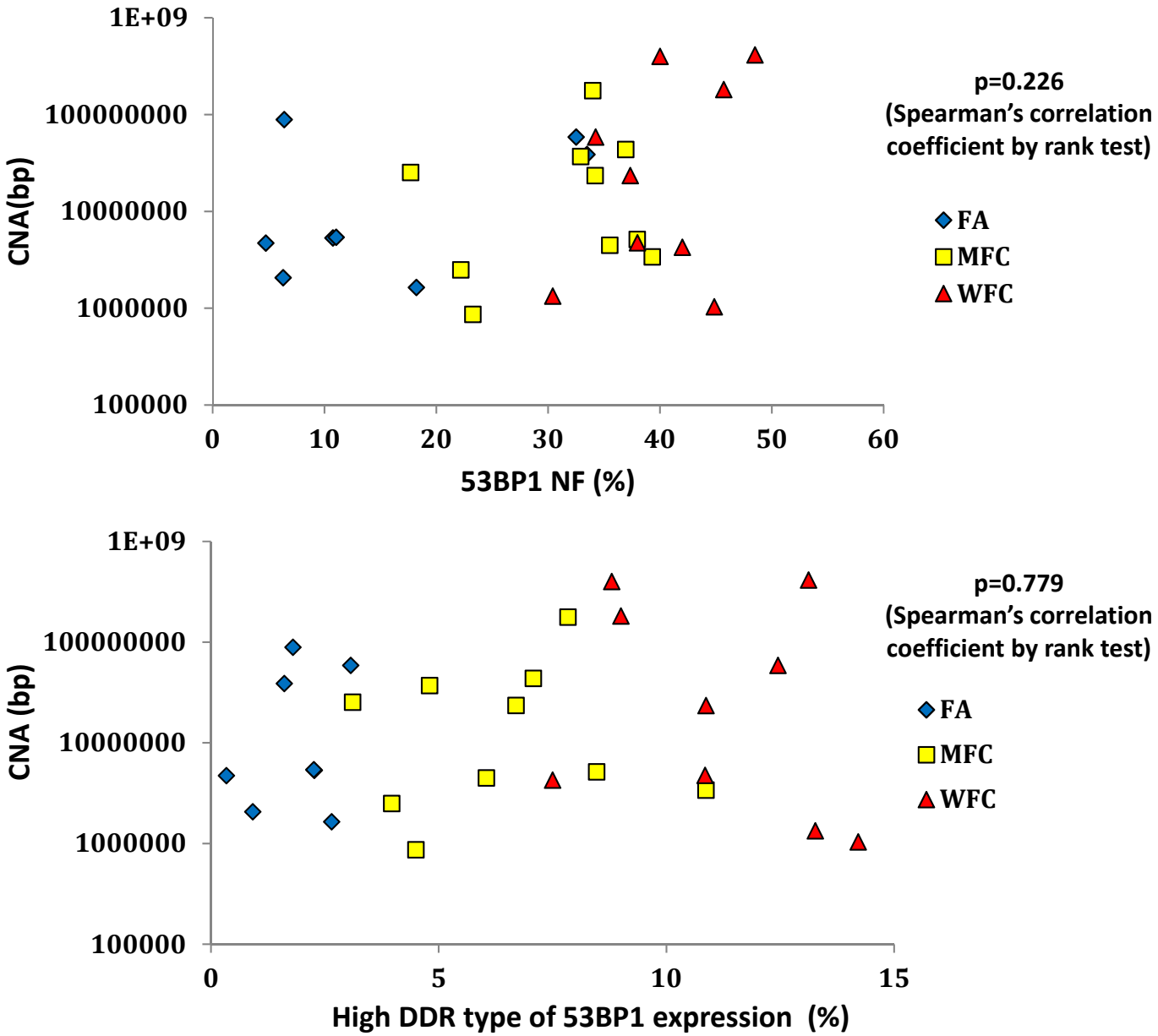
1E+09
100000000
10000000
1000000
100000
CNA(bp)
0
10
20
30
40
50
60
53BP1 NF (%)
p=0.226
(Spearman's correlation coefficient by rank test)
FA
MFC
WFC
1E+09
100000000
10000000
1000000
100000
CNA (bp)
0
5
10
15
High DDR type of 53BP1 expression (%)
p=0.779
(Spearman's correlation coefficient by rank test)
FA
MFC
WFC

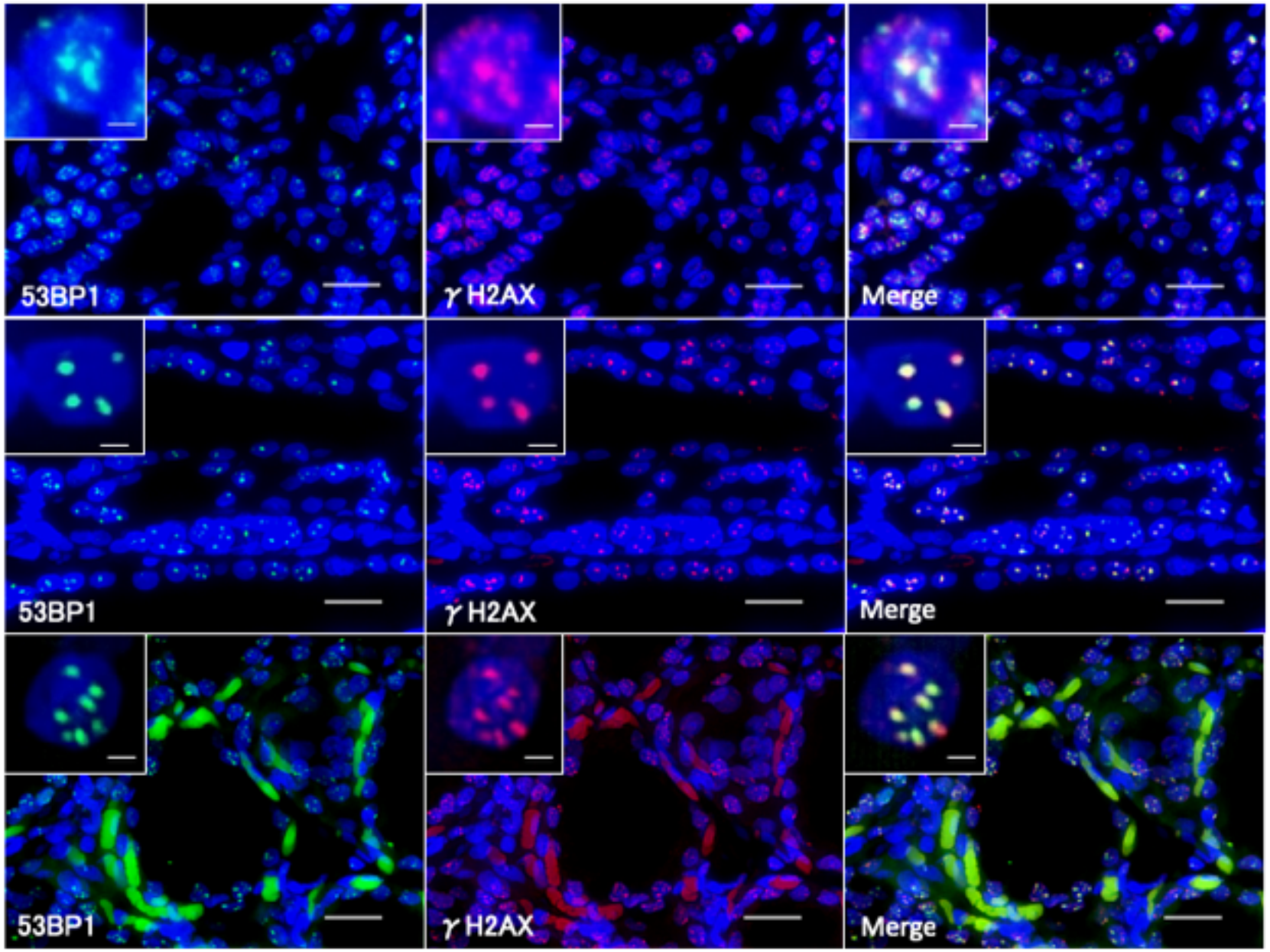
53BP1
γ H2AX
Merge
53BP1
γ H2AX
Merge
53BP1
γ H2AX
Merge